

Quantum spin-transfer torque induced nonclassical magnetization dynamics and electron-magnetization entanglement

Priyanka Mondal,¹ Marko D. Petrović,² Petr Plecháč,² and Branislav K. Nikolić^{1,*}

¹*Department of Physics and Astronomy, University of Delaware, Newark, DE 19716, USA*

²*Department of Mathematical Sciences, University of Delaware, Newark, DE 19716, USA*

The standard spin-transfer torque (STT)—where spin-polarized current drives dynamics of magnetization viewed as a classical vector—requires noncollinearity between electron spins carried by the current and magnetization of a ferromagnetic layer. However, recent experiments [A. Zholud *et al.*, Phys. Rev. Lett. **119**, 257201 (2017)] observing magnetization dynamics in spin valves at cryogenic temperatures, even when electron spin is collinear to magnetization, point at overlooked quantum effects in STT which can lead to *highly nonclassical* magnetization states. Using fully quantum many-body treatment, where an electron injected as spin-polarized wave packet interacts with local spins comprising the anisotropic quantum Heisenberg ferromagnetic chain, we define *quantum STT as any time evolution of local spins due to initial many-body state not being an eigenstate of electron+local-spins system*. For time evolution caused by injected spin- \downarrow electron scattering off local \uparrow -spins, *entanglement* between electron subsystem and local spins subsystem takes place leading to *decoherence* and, therefore, shrinking of the total magnetization but without rotation from its initial orientation which explains the experiments. Furthermore, the same processes—entanglement and thereby induced decoherence—are present also in standard noncollinear geometry, together with the usual magnetization rotation. This is because STT in quantum many-body picture is caused only by electron spin- \downarrow factor state, and the only difference between collinear and noncollinear geometries is in relative size of the contribution of the initial separable state containing such factor state to superpositions of separable many-body quantum states generated during time evolution.

The standard spin-transfer torque (STT) [1], predicted in the seminal work of Slonczewski [2] and Berger [3], is a phenomenon where a flux of spin-polarized electrons injected into a ferromagnetic metal (FM) layer drives its magnetization dynamics. The origin of STT is transfer of spin angular momentum from electrons to local magnetic moments of the FM layer, so it is fundamentally a nonequilibrium quantum many-body physics effect. Nevertheless, local magnetic moments are typically treated as *classical vectors of fixed length* [1, 4] whose dynamics is governed by the Landau-Lifshitz-Gilbert (LLG) equation [5] extended by adding the STT term [6–8]

$$\mathbf{T} \propto \langle \hat{\mathbf{s}}_e \rangle \times \mathbf{S}(\mathbf{r}). \quad (1)$$

Thus, the nonequilibrium spin density $\langle \hat{\mathbf{s}}_e \rangle$ caused by flowing electrons *must be noncollinear* to the direction of local spin $\mathbf{S}(\mathbf{r})$ [i.e., to the local magnetization proportional to local spin], to drive magnetization dynamics in such a classical picture. The dynamics can include oscillations or complete reversal, whose conversion into resistance variations has emerged as a key resource for next generation spintronic technologies, such as nonvolatile magnetic random access memories, microwave oscillators, microwave detectors, spin-wave emitters, memristors and artificial neural networks [9–11].

For example, passing current through a spin valve tri-layer fixed-FM/normal-metal/free-FM, as employed in early experiments on standard STT [12, 13], causes first FM layer with fixed magnetization to spin-polarize the current which then impinges onto the second FM layer with free magnetization that fluctuates in the classical picture due to a random magnetic field caused by thermal

motion. When impinging spins and fluctuating magnetization become noncollinear, standard STT can either amplify such fluctuations (for fixed-to-free spin current direction) or reduce them (for free-to-fixed spin current direction), as confirmed theoretically [14] and experimentally [15] at room temperature.

However, this well-established picture *cannot* explain very recent experiments [16] on collinear spin valves at cryogenic temperatures $\lesssim 3$ K, where resistance measurements have revealed magnetization dynamics even though thermal fluctuations that could introduce noncollinearity between the free and fixed magnetizations are suppressed. This implies a mechanism where standard STT is zero, $\mathbf{T} = 0$ in Eq. (1), so that magnetization does not rotate from the the initial configuration. Nevertheless, it changes its length, thereby signaling generation of *highly nonclassical* magnetization states [16]. However, the proposed intuitive picture [16] where such mechanism would amplify quantum spin fluctuations, for both fixed-to-free and free-to-fixed spin current directions, cannot be rigorously justified. That is, although quantum fluctuations of the local spin operators [17] (or, equivalently, zero-point energy of magnons as bosonic particles to which spin operators can be mapped) play an important role in lowering the energy of classical ground states of antiferromagnets [18] or noncollinear spin textures [19], they *vanish* in a FM with uniaxial anisotropy because the collinear state of local magnetic moments is also a ground eigenstate of the exact Hamiltonian [20].

Aside from few disparate attempts [21–23], a general framework for describing current-driven *quantum dynamics* of magnetization is lacking. Note that quantum trans-

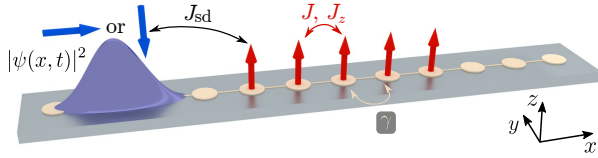


FIG. 1. Schematic view of a quantum many-body system, exhibiting quantum STT, which consists of a FM layer whose local spins comprise the XXZ quantum Heisenberg ferromagnetic chain with anisotropic exchange interactions J and J_z , and are attached to 1D TB chain where electron hops with parameter γ . The spin-polarized electron wave packet is injected along the TB chain, with its spin pointing in the $-z$ - or $+x$ -direction which is collinear (a case where standard STT of Slonczewski [2] and Berger [3] is absent) or noncollinear, respectively, to local spins pointing initially along the $+z$ -direction. The spin of the wave packet interacts with local spins via s - d exchange interaction.

port theories, such as the nonequilibrium Green function formalism [7, 8, 24, 25] or the scattering matrix approach [26, 27], are routinely used to compute $\langle \hat{s}_e \rangle$ in Eq. (1) for a given single-particle Hamiltonian, but this serves only as an input [7, 8] for the LLG equation describing classical dynamics of magnetization. The LLG equation can be justified under the assumptions [5] of large spin $S \rightarrow \infty$, $\hbar \rightarrow 0$ (while $S \times \hbar \rightarrow 1$) and in the *absence of entanglement*. The latter assumption means that local spins comprising the total magnetization should remain in a separable quantum state, $|S_1\rangle \otimes |S_2\rangle \otimes \dots \otimes |S_N\rangle$, as exemplified by the ground state of FM, $|\uparrow\rangle \otimes |\uparrow\rangle \otimes \dots \otimes |\uparrow\rangle$.

Instead of classical micromagnetics [4, 14] or quantum-classical [7, 8] description of standard-STT-induced magnetization dynamics, here we introduce a quantum many-body picture of *both* flowing-electron-spin-local-spins interactions and the ensuing time evolution of local spins at zero temperature. For this purpose, we employ a system depicted in Fig. 1 where spin-polarized electron wave packet, assumed to originate from a fixed FM layer, is injected along one-dimensional (1D) tight-binding (TB) chain whose sites in the middle host local spins comprising a quantum Heisenberg ferromagnetic chain modeling the free FM layer. The states of such composite quantum system electron+local-spins reside in the Hilbert space

$$\mathcal{H} = \mathcal{H}_{\text{orb}}^e \otimes \mathcal{H}_{\text{spin}}^e \otimes \mathcal{H}_{\text{spin}}^1 \otimes \dots \otimes \mathcal{H}_{\text{spin}}^N, \quad (2)$$

which is the tensor product of orbital electron subspace $\mathcal{H}_{\text{orb}}^e$ (of finite dimension equal to the number of sites of the TB chain); two-dimensional subspace $\mathcal{H}_{\text{spin}}^e$ for electron spin; and $\mathcal{H}_{\text{spin}}^n$ as two-dimensional subspaces for $n = 1, \dots, N$ local spins assumed to be spin- $\frac{1}{2}$ as

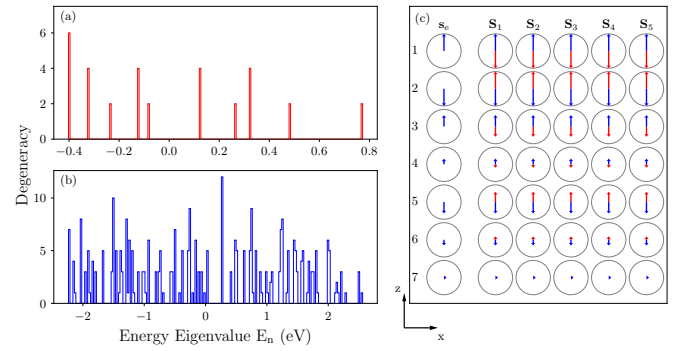


FIG. 2. (a) Eigenspectrum of the XXZ quantum Heisenberg ferromagnetic chain whose $N = 5$ local spins in Fig. 1 do not interact with electron spin ($J_{sd} = 0$). (b) Eigenspectrum of many-body Hamiltonian in Eq. (3) whose local spins interact via s - d interaction ($J_{sd} = 0.1$ eV) with electron spin on TB site i . (c) Expectation value of electron spin (first column) and local spins, extracted from their subsystem density matrices via Eq. (6), in the degenerate ground state of the lowest energy in panel (a) [red arrows] or (b) [blue arrows].

well. The system Hamiltonian acting in \mathcal{H} is

$$\hat{H} = -\gamma \sum_{\langle ij \rangle} |i\rangle\langle j| - J_{sd} \sum_i |i\rangle\langle i| \otimes \hat{s}_e \cdot \hat{\mathbf{s}}_i(t) - \sum_{\langle ij \rangle} \left[J(\hat{S}_i^x \cdot \hat{S}_j^x + \hat{S}_i^y \cdot \hat{S}_j^y) + J_z \hat{S}_i^z \cdot \hat{S}_j^z \right], \quad (3)$$

where $|i\rangle$ is electron orbital centered on site i ; $\gamma = 1$ eV is hopping between nearest-neighbor sites; and $J_{sd} = 0.1$ eV is the strength of s - d exchange interaction between electron and local spins. The exchange interaction between the nearest neighbor local spins is $J = 0.1$ eV and $J_z = 0.1005$ eV, which are slightly different in order to include the uniaxial anisotropy. The third term in Eq. (3) is standardly denoted as the XXZ quantum Heisenberg ferromagnetic chain [28, 29]. The spin operators in Eq. (3) are constructed as $\hat{s}_e = \hat{I} \otimes \hat{\sigma} \otimes \hat{I} \otimes \dots \otimes \hat{I}$ for electron spin; $\hat{\mathbf{s}}_i = \hat{I} \otimes \hat{I} \otimes \hat{\sigma} \otimes \hat{I} \otimes \dots \otimes \hat{I}$ for first local spins and analogously for all other local spins, where $\hat{\sigma} = (\hat{\sigma}_x, \hat{\sigma}_y, \hat{\sigma}_z)$ is the vector of the Pauli matrices and \hat{I} is the unit operator. The eigenspectrum of an isolated XXZ chain (i.e., of the third term in Eq. (3) alone) is shown in Fig. 2(a), while the eigenspectrum of the whole many-body Hamiltonian in Eq. (3) is shown in Fig. 2(b). The ground state in the former (latter) case has degeneracy six (seven), as expected for coupled system of five (six) spin- $\frac{1}{2}$ [28].

At $t = 0$, the many-body quantum state is a separable one

$$\langle x|\Psi(t=0)\rangle = Ce^{ik_xx - \delta k_x^2 x^2/4} \otimes \chi_e \otimes \chi_1 \otimes \dots \otimes \chi_N. \quad (4)$$

Its first factor is electron orbital quantum state in $\mathcal{H}_{\text{orb}}^e$ chosen as a Gaussian wave packet with momentum along the $+x$ -direction and centered on the left edge of TB

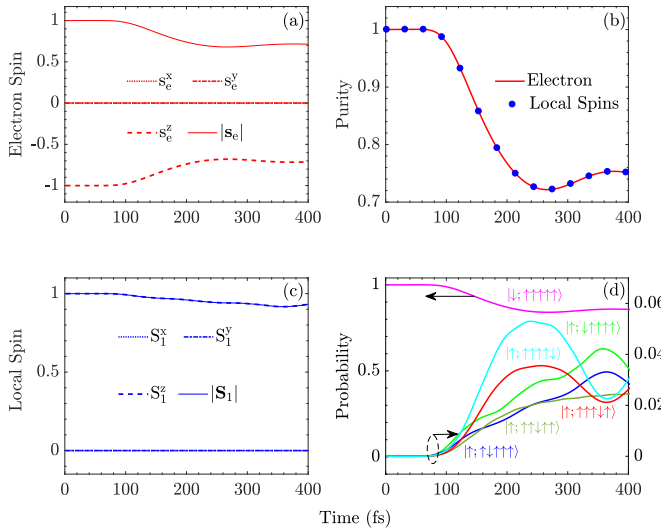


FIG. 3. Time dependence of the expectation value of spin (in units $\hbar/2$) obtained from spin- $\frac{1}{2}$ density matrix in Eq. (6) for: (a) spin of injected electron wave packet in Fig. 1 which at $t = 0$ points in the $-z$ -direction that is *collinear* and antiparallel to local spins pointing in the $+z$ -direction; and (c) first local spin in Fig. 1 [time dependence of expectation value of local spins $n = 2-5$ is nearly identical to (c)]. (b) Purity defined in Eq. (7) of the subsystem composed of electron degrees of freedom (orbital and spin) or of the subsystem composed of all local spins. (d) Probability in Eq. (8) to find electron-spin+local-spins subsystem in many-body quantum state $|\sigma_e; \sigma_1 \sigma_2 \sigma_3 \sigma_4 \sigma_5\rangle$.

chain, as illustrated in Fig. 1, where C is the normalization constant. To mimic current of electrons at the Fermi level which interact with the ground state of free FM layer within a spin valve, we use $k_x a = 0.1$ and $\delta k_x a = 0.2$ (a is the lattice spacing) which specify average energy $E = -2.36$ eV and its standard deviation $\delta E = 0.054$ eV for the wave packet to be close to the ground state eigenenergy $E_0 = -2.43$ eV [Fig. 2(b)] of the Hamiltonian in Eq. (3). In the ground state, all local spins are aligned with the anisotropy z -axis, as shown in Fig. 2(c), so we choose $\chi_n = \begin{pmatrix} 1 \\ 0 \end{pmatrix}$ for $n = 1, \dots, N$. To mimic minority electrons in spin valve with collinear magnetizations impinging on the free FM layer, we select initial spin polarization of the wave packet in the $-z$ -direction, as described by the spinor $\chi_e = \begin{pmatrix} 0 \\ 1 \end{pmatrix}$. For standard STT setup with noncollinear magnetizations of the FM layers, we use spin polarization in the $+x$ -direction, $\chi_e = \frac{1}{\sqrt{2}} \begin{pmatrix} 1 \\ 1 \end{pmatrix}$.

Although many-body quantum system depicted in Fig. 1 could be evolved via time-dependent density matrix renormalization group [30] for large number of local spins ~ 100 , for transparency of our discussion, operating with small number of excited states of the XXZ chain

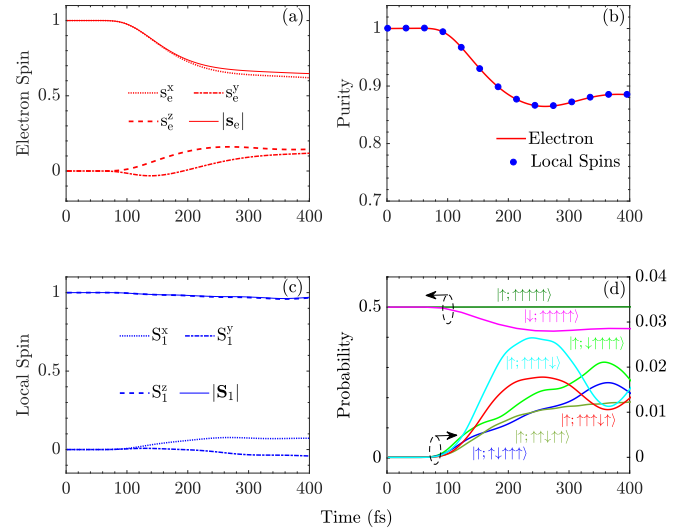


FIG. 4. Panels (a)–(d) plot the same information as panels (a)–(d), respectively, in Fig. 3 but for injected electron wave packet which at $t = 0$ is spin-polarized in the $+x$ -direction, i.e., *noncollinear* to local spins pointing in the $+z$ -direction.

which can be analyzed one by one, we employ $N = 5$ local spins. The chosen length $L_x = 400$ of the TB chain ensures that wave packet does not reflect from its boundaries within the time frame considered in Figs. 3 and 4. The *numerically exact* $|\Psi(t)\rangle$, governed by the Schrödinger equation $i\hbar\partial|\Psi(t)\rangle/\partial t = \hat{H}|\Psi(t)\rangle$, is obtained by using the Crank-Nicolson algorithm [31].

Figure 2(c) shows that degenerate ground state has electron and local spins parallel to each other due to s - d interaction between them acting to align them. Thus, when an electron with spin- \downarrow along the $-z$ -direction is injected, its spin is collinear to local spins but $|\Psi(t=0)\rangle = |G\rangle \otimes |\downarrow_e; \uparrow_1 \dots \uparrow_N\rangle$ (this form is used below for economy of notation) at $t = 0$ is not an eigenstate of the Hamiltonian in Eq. (3). *This causes time evolution of the electron-spin+local-spins subsystem, which rigorously defines quantum STT even in situation where standard STT in Eq. (1) is identically zero.* In the course of time evolution, $|\Psi(t)\rangle$ becomes an entangled state due to linear superpositions of separable states being generated for $t > 0$. The entanglement entails that each subsystem must be described using the appropriate reduced density matrix [32]

$$\hat{\rho}_{\text{sub}} = \text{Tr}_{\text{other}}|\Psi(t)\rangle\langle\Psi(t)|, \quad (5)$$

obtained via partial trace applied to the pure state density matrix $|\Psi(t)\rangle\langle\Psi(t)|$. For example, tracing over the states in the subspace $\mathcal{H}_{\text{orb}}^e \otimes \mathcal{H}_{\text{spin}}^e \mathcal{H}_{\text{spin}}^2 \dots \otimes \mathcal{H}_{\text{spin}}^N$ yields the density matrix of first local spin

$$\hat{\rho}_1(t) = \frac{1}{2} \left[\hat{I} + \mathbf{S}_1(t) \cdot \hat{\boldsymbol{\sigma}} \right], \quad (6)$$

where $\mathbf{S}_1(t) = \text{Tr}[\hat{\rho}_1(t)\hat{\boldsymbol{\sigma}}]$ is the spin expectation value

(in units of $\hbar/2$), also denoted as the polarization (or Bloch) vector [32]. Pure (or fully coherent) quantum states of spin- $\frac{1}{2}$ are characterized by $|\mathbf{S}_1| = 1$, while $0 < |\mathbf{S}_1| < 1$ signifies their decoherence [32, 33] toward mixed (or partially coherent [34]) states. Figure 3(c) shows that first local spin has $S_1^z < 1$, $S_1^x = S_1^y \equiv 0$ and, therefore, $|\mathbf{S}_1| < 1$. The electron spin also exhibits decoherence, $|\mathbf{s}_e| < 1$, in Fig. 3(a). Virtually the same time-dependences as in Fig. 3(c) are obtained for other local spins $i = 2, \dots, 5$, and, therefore, for total magnetization as the sum of local spins. Thus, this could be precisely the highly nonclassical state of magnetization conjectured from the measurement of the spin valve resistance [16], which increases $\propto 1 - M_z$ due to magnetization $M_z = g\mu_B \sum_i S_i^z$ shrinking without rotation (i.e., $M_x = M_y = 0$) away from its initial orientation.

To explain the origin of magnetization decoherence, or, equivalently, of the subsystem comprised of *all* local spins, we view multipartite [due to $N + 2$ factors in Eq. (2)] total system as a bipartite one, i.e., as being composed of the electron subsystem with states residing in $\mathcal{H}_{\text{orb}}^e \otimes \mathcal{H}_{\text{spin}}^e$ and the subsystem of local spins. The purity of the former is defined as [32, 33]

$$\mathcal{P}_{\text{spins}}^{\text{local}}(t) = \text{Tr} \{ [\hat{\rho}_{\text{spins}}^{\text{local}}(t)]^2 \}, \quad (7)$$

where density matrix $\hat{\rho}_{\text{spins}}^{\text{local}}(t)$ is obtained via Eq. (5) by tracing over the states in the subspace $\mathcal{H}_{\text{orb}}^e \otimes \mathcal{H}_{\text{spin}}^e$. The decay of $\mathcal{P}_{\text{spins}}^{\text{local}}(t)$ below one in Fig. 3(b) quantifies “true decoherence” [33] of initially pure state $|\uparrow\rangle \otimes |\uparrow\rangle \otimes \dots \otimes |\uparrow\rangle$ as the decay [32, 33] of the off-diagonal elements of $\hat{\rho}_{\text{spins}}^{\text{local}}(t)$ caused by entanglement with the electron subsystem. The purity of decohered electron subsystem in Fig. 3(b) is identical to that of the local spin subsystem, as expected for entanglement in bipartite quantum systems [32, 33].

To understand the states of electron-spin+local-spins subsystem which are excited during time evolution initiated by injection of a single spin-polarized electron, we compute the density matrix $\hat{\rho}_{\text{spins}}^{\text{e+local}}(t)$ of this subsystem obtained by partial trace in Eq. (5) performed over the states in $\mathcal{H}_{\text{orb}}^e$. The probability to find this subsystem in state $|\sigma_e; \sigma_1 \dots \sigma_N\rangle$ at time t

$$\text{prob}_{\text{spins}}^{\text{e+local}}(t) = \langle \sigma_e; \sigma_1 \dots \sigma_N | \hat{\rho}_{\text{spins}}^{\text{e+local}}(t) | \sigma_e; \sigma_1 \dots \sigma_N \rangle, \quad (8)$$

is shown in Fig. 3(d) for electron injected with spin along the $-z$ -direction. The subspace of \mathcal{H} whose states can generate nonzero $\text{prob}_{\text{spins}}^{\text{e+local}}(t)$ is restricted by energy bands in Fig. 2(b) [caused by anisotropy and boundaries [29]] and symmetries, such as that total spin in the z -direction has to be conserved in time evolution due to operator $\hat{S}_{\text{tot}}^z = \hat{s}^z + \hat{S}_1^z + \dots + \hat{S}_N^z$ commuting with the Hamiltonian in Eq. (3), $[\hat{H}, \hat{S}_{\text{tot}}^z] = 0$. Because of the latter requirement, all states $|\sigma_e; \sigma_1 \dots \sigma_N\rangle$ participating in time evolution must have the same number of \uparrow -spins,

so that one finds in Fig. 3(d) progressive excitation of states with flipped spin of electron and one flipped local spin with transfer of angular momentum of $1 \times \hbar$. However, the initial state $|\downarrow; \uparrow \dots \uparrow\rangle$ maintains its probability close to one, and other states with flipped electron spin and one flipped local spin have much smaller and nonuniform probability. Such peculiar quantum superposition of separable many-body states, with large contribution from the initial state, leads to local spins maintaining their direction along the z -axis in Fig. 3(c). This can be contrasted with naïve (i.e., not taking into account superpositions) intuition [22, 35] where spin- \downarrow electron simply flips first local spin—the flip then propagates to displace transversally other local spins away from the anisotropy axis, eventually exciting white spectrum [22] of lowest spin waves modes [28] (where total spin is lower than that of the ground state by $1 \times \hbar$) of the free FM layer.

The same effects—entanglement of electron state and state of all local spins [Fig. 4(b)]; thereby induced decoherence of electron spin [Fig. 4(a)] and local spins [Fig. 4(c)]; and high probability [Fig. 4(d)] to find initial state of electron-spin+local-spins subsystem in the course of time evolution—is present also in standard STT geometry with noncollinearity between spin of injected electron and local spins. Furthermore, probabilities $\text{prob}_{\text{spins}}^{\text{e+local}}(t)$ in Fig. 4(d) to excite states of type $|\uparrow; \uparrow \dots \downarrow \dots \uparrow\rangle$ are simply half of those obtained for collinear geometry in Fig. 3(d) since spin of injected electron along the $+x$ -direction used in Fig. 4 means $|\rightarrow_e\rangle = \frac{1}{\sqrt{2}}(|\uparrow_e\rangle + |\downarrow_e\rangle)$ where only $\frac{1}{\sqrt{2}}|\downarrow_e\rangle$ term, entering as a factor of the initial many-body state $|G\rangle \otimes \frac{1}{\sqrt{2}}(|\uparrow_e\rangle + |\downarrow_e\rangle) \otimes |\uparrow_1 \dots \uparrow_N\rangle$, induces time evolution of local spins and transfer of angular momentum. On the other hand, $\frac{1}{\sqrt{2}}|\uparrow_e\rangle \otimes |\uparrow_1 \dots \uparrow_N\rangle$ term in the initial many-body state is an eigenstate [Fig. 2(c)] of electron-spin+local-spins subsystem and, therefore, has $\text{prob}_{\text{spins}}^{\text{e+local}}(t) = 1/2$ which does not evolve in time in Fig. 4(d). Thus, identical profile of curves in Figs. 3(d) and 4(d) reveal that *in fully quantum many-body picture there is no difference between standard STT and quantum STT*—both require $|\downarrow_e\rangle$ factor state in the initial many-body state, where such factor is due to electron spin state (in the collinear case) or a term in the superposition of electron spin states (in the noncollinear case).

Note added.—During the completion of this work, we became aware of two studies [36, 37] where magnetization dynamics in collinear spin valves at cryogenic temperatures is attributed to current-enhanced quantum spin fluctuations. However, as discussed above, such fluctuations are forbidden in the ground state of ferromagnets [20], and if generated as random magnetic field [38] by the nonequilibrium spin shot noise [36], they would lead to rotation of magnetization away from the initial collinear direction that was excluded from the experiments of Ref. [16]. We propose to clarify the role of

spin shot noise by using a sequence of Lorentzian voltage pulses to inject a train of levitons into a collinear spin valve, where leviton as a minimal collective many-body excitation above the Fermi sea carrying a single electron charge, is free of particle-hole pairs and has vanishing current noise [39, 40].

We are grateful to S. Urazhdin for instructive discussions. P. M. and B. K. N. were supported by NSF Grant No. ECCS 150909. M. P. and P. P. were supported by ARO MURI Award No. W911NF-14-0247.

* bnikolic@udel.edu

- [1] D. Ralph and M. Stiles, Spin transfer torques, *J. Magn. Magn. Mater.* **320**, 1190 (2008).
- [2] J. C. Slonczewski, Current-driven excitation of magnetic multilayers, *J. Magn. Magn. Mater.* **159**, L1 1996.
- [3] L. Berger, Emission of spin waves by a magnetic multilayer traversed by a current, *Phys. Rev. B* **54**, 9353 (1996).
- [4] D. V. Berkov and J. Miltat, Spin-torque driven magnetization dynamics: Micromagnetic modeling, *J. Magn. Magn. Mater.* **320**, 1238 (2008).
- [5] R. Wieser, Description of a dissipative quantum spin dynamics with a Landau-Lifshitz-Gilbert like damping and complete derivation of the classical Landau-Lifshitz equation, *Euro. Phys. J. B* **88**, 77 (2015).
- [6] A. Manchon, N. Ryzhanova, A. Vedyayev, M. Chschiev, and B. Dieny, Description of current-driven torques in magnetic tunnel junctions, *J. Phys.: Condens. Matter* **20**, 145208 (2008).
- [7] M. D. Petrović, B. S. Popescu, U. Bajpai, P. Plecháč, and B. K. Nikolić, Spin and charge pumping by steady or pulse current-driven magnetic domain wall: A self-consistent multiscale time-dependent-quantum/time-dependent-classical approach, [arXiv:1802.05682](https://arxiv.org/abs/1802.05682) (2018).
- [8] M. O. A. Ellis, M. Stamenova, and S. Sanvito, Multiscale modeling of current-induced switching in magnetic tunnel junctions using *ab initio* spin-transfer torques, *Phys. Rev. B* **96**, 224410 (2017).
- [9] N. Locatelli, V. Cros, and J. Grollier, Spin-torque building blocks, *Nat. Mater.* **13**, 11 (2014).
- [10] A. D. Kent and D. C. Worledge, A new spin on magnetic memories, *Nat. Nanotech.* **10**, 187 (2015).
- [11] W. A. Borders, H. Akima, S. Fukami, S. Moriya, S. Kurihara, Y. Horio, S. Sato, and H. Ohno, Analogue spinorbit torque device for artificial-neural-network-based associative memory operation, *Appl. Phys. Expr.* **10**, 013007 (2017).
- [12] M. Tsoi, A. G. M. Jansen, J. Bass, W. C. Chiang, V. Tsoi, and P. Wyder, Generation and detection of phase-coherent current-driven magnons in magnetic multilayers, *Nature* **406**, 46 (2000).
- [13] J. A. Katine, F. J. Albert, R. A. Buhrman, E. B. Myers, and D. C. Ralph, Current-driven magnetization reversal and spin-wave excitations in Co/Cu/Co pillars, *Phys. Rev. Lett.* **84**, 3149 (2000).
- [14] Z. Li and S. Zhang, Thermally assisted magnetization reversal in the presence of a spin-transfer torque, *Phys. Rev. B* **69**, 134416 (2004).
- [15] R. H. Koch, J. A. Katine, and J. Z. Sun, Time-resolved reversal of spin-transfer switching in a nanomagnet, *Phys. Rev. Lett.* **92**, 088302 (2004).
- [16] A. Zholud, R. Freeman, R. Cao, A. Srivastava, and S. Urazhdin, Spin transfer due to quantum magnetization fluctuations, *Phys. Rev. Lett.* **119**, 257201 (2017).
- [17] Y. Takahashi, *Spin Fluctuation Theory of Itinerant Electron Magnetism* (Springer, Berlin, 2013).
- [18] A. Singh and Z. Tešanović, Quantum spin fluctuations in an itinerant antiferromagnet, *Phys. Rev. B* **41**, 11457 (1990).
- [19] A. Roldán-Molina, M. J. Santander, A. S. Núñez, and J. Fernández-Rossier, Quantum fluctuations stabilize skyrmion textures, *Phys. Rev. B* **92**, 245436 (2015).
- [20] K. Yosida, *Theory of Magnetism* (Springer, Berlin, 1996).
- [21] Y. Wang and L. J. Sham, Quantum dynamics of a nanomagnet driven by spin-polarized current, *Phys. Rev. B* **85**, 092403 (2012); Y. Wang, and L. J. Sham, Quantum approach of mesoscopic magnet dynamics with spin transfer torque, *Phys. Rev. B* **87**, 174433 (2013); T. Tay and L. J. Sham, Theory of atomistic simulation of spin-transfer torque in nanomagnets, *Phys. Rev. B* **87**, 174407 (2013).
- [22] J. P. Gauyacq and N. Lorente, Excitation of spin waves by tunneling electrons in ferromagnetic and antiferromagnetic spin- $\frac{1}{2}$ Heisenberg chains, *Phys. Rev. B* **83**, 035418 (2011); J. P. Gauyacq and N. and Lorente, Magnetic reversal of a quantum nanoferromagnet, *Phys. Rev. B* **87**, 195402 (2013).
- [23] F. Mahfouzi and N. Kioussis, Current-induced damping of nanosized quantum moments in the presence of spin-orbit interaction, *Phys. Rev. B* **95**, 184417 (2017).
- [24] P. M. Haney, D. Waldron, R. A. Duine, A. S. Núñez, H. Guo, and A. H. MacDonald, Current-induced order parameter dynamics: Microscopic theory applied to Co/Cu/Co spin valves, *Phys. Rev. B* **76**, 024404 (2007).
- [25] B. K. Nikolić, K. Dolui, M. Petrović, P. Plecháč, T. Markussen, and K. Stokbro, First-principles quantum transport modeling of spin-transfer and spin-orbit torques in magnetic multilayers, [arXiv:1801.05793](https://arxiv.org/abs/1801.05793) (2018).
- [26] M. D. Stiles and A. Zangwill, Anatomy of spin-transfer torque, *Phys. Rev. B* **66**, 014407 (2002).
- [27] S. Wang, Y. Xu, and K. Xia, First-principles study of spin-transfer torques in layered systems with noncollinear magnetization, *Phys. Rev. B* **77**, 184430 (2008).
- [28] J. B. Parkinson and D. J. J. Farnell, *An Introduction to Quantum Spin Systems* (Springer, Berlin, 2010).
- [29] K. Joel, D. Kollmar, and L. F. Santos, An introduction to the spectrum, symmetries, and dynamics of spin-1/2 Heisenberg chains, *Am. J. Phys.* **81**, 450 (2013).
- [30] U. Schollwöck, The density-matrix renormalization group, *Rev. Mod. Phys.* **77**, 259 (2005).
- [31] J. E. Bayfield, *Quantum Evolution: An Introduction to Time-Dependent Quantum Mechanics* (Wiley, New York, 1999).
- [32] L. E. Ballentine, *Quantum Mechanics: A Modern Development* (World Scientific, Singapore, 2014).
- [33] E. Joos, H. D. Zeh, C. Kiefer, D. J. W. Giulini, J. Kupsch, and I. Stamatescu, *Decoherence and the Appearance of a Classical World in Quantum Theory* (Springer, Berlin, 2003).
- [34] B. K. Nikolić and S. Souma, Decoherence of transported spin in multichannel spin-orbit-coupled spintronic de-

vices: Scattering approach to spin-density matrix from the ballistic to the localized regime, *Phys. Rev. B* **71**, 195328 (2005).

[35] T. Balashov, A. F. Takács, M. Däne, A. Ernst, P. Bruno, and W. Wulfhekel, Inelastic electron-magnon interaction and spin transfer torque, *Phys. Rev. B* **78**, 174404 (2008).

[36] A. Qaiumzadeh and A. Brataas, Quantum population of magnons via spin shot noise, [arXiv:1808.02907](https://arxiv.org/abs/1808.02907) (2018).

[37] S. A. Bender, R. A. Duine, and Y. Tserkovnyak, Quantum spin-transfer torque and magnon-assisted transport in nanostructures, [arXiv:1808.00777](https://arxiv.org/abs/1808.00777) (2018).

[38] A. L. Chudnovskiy, J. Swiebodzinski, and A. Kamenev, Spin-torque shot noise in magnetic tunnel junctions, *Phys. Rev. Lett.* **101**, 066601 (2008).

[39] J. Keeling, I. Klich, and L. S. Levitov, Minimal excitation states of electrons in one-dimensional wires, *Phys. Rev. Lett.* **97**, 116403 (2006).

[40] J. Dubois, T. Jullien, F. Portier, P. Roche, A. Cavanna, Y. Jin, W. Wegscheider, P. Roulleau, and D. C. Glattli, Minimal-excitation states for electron quantum optics using levitons, *Nature* **502**, 659 (2013).